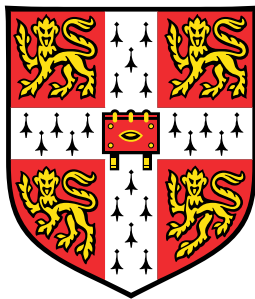


Mitigating the effects of air bubbles on glider data to investigate productivity around Southern Ocean seamounts



Louis De Neve

Department of Applied Maths and Theoretical Physics
University of Cambridge

This thesis is submitted for the degree of
Master in Science

Easter 2025

Word count: 7098

Mitigating the effects of air bubbles on glider data to investigate productivity around Southern Ocean seamounts

Abstract

Phytoplankton-driven biological productivity influences carbon sequestration from the surface into the deep ocean. By using buoyancy glider data from Discovery Bank in the South Scotia Ridge, this thesis investigates the impact of Taylor columns, hydrodynamic structures that form around seamounts, on this productivity. Air bubbles in water present a challenge to glider based bio-optical measurements by artificially inflating particulate backscattering coefficient readings, on the downward portion of the glider path. This thesis presents a novel method for mitigating the impact of bubbles on this data by applying a correction based on nearby unaffected upcasts, reducing the difference between up and downcasts by a factor of 6. The corrected data then reveals regions where high chlorophyll concentrations extend beyond the photic depth. These regions occur along the boundaries of the proposed Taylor column location, indicating increased nutrient upwelling and enhanced diapycnal mixing. The centre of the column does not show this effect, suggesting that increased water residence time in the centre of the column competes with the enhanced diapycnal mixing to limit nutrient availability and productivity. The findings suggest that the Taylor column significantly affects the productivity around Discovery Bank, highlighting the importance of accurate carbon sinking flux calculations to inform global climate policy decisions.

1. Introduction

With the ocean containing 60 times as much carbon as the atmosphere (DeVries, 2022), a thorough understanding of oceanic systems is needed to help guide climate policy decisions. The flux of carbon down into the deep ocean affects how much carbon is stored within the ocean, with the most significant factor affecting this being the primary productivity of phytoplankton, by which CO₂, or its derivatives, is converted into Particulate Organic Carbon (POC) (Eppley, Renger, and Betzer, 1983). This primary biological productivity (hereafter referred to as "productivity") is in turn affected by a multitude of factors including temperature, the biota present in a region and the availability of key nutrients - within the Southern Ocean the primary limiting nutrient is iron (Vives et al., 2022). Hydrodynamic structures can have an effect on productivity by changing the availability of these key nutrients. Taylor columns are a fluid dynamic phenomenon where the perturbation of a rotating fluid by a solid body creates rotating columns parallel to the rotation axis (Fuentes, 2009). In the ocean, these columns can form around seamounts, large underwater mountains that do not breach the surface. Taylor columns have been shown to affect the mixing of the ocean around seamounts (Meredith et al., 2015). Increased vertical mixing within the column results in more nutrients from below the euphotic zone being brought up towards the surface, increasing productivity (Ellison, 2023). This thesis aims to clarify the effect that undersea topography has on this productivity by investigating the change in chlorophyll- α (henceforth referred to as "chlorophyll") concentrations and sinking particulate matter across transects over Discovery Bank, one of the largest seamounts in the South Scotia Ridge.

The vast size of the ocean makes studying these systems incredibly difficult. Within the Southern Ocean this problem is compounded by harsh weather and sea conditions, further exaggerated during the austral winter. In the past decade, buoyancy gliders have been utilised to acquire ocean data across broad temporal and spatial ranges throughout the Southern Ocean. Buoyancy gliders have recently become key tools for oceanographers to investigate biological and hydrodynamic systems within seas and oceans. Similar to the Argo float programme (Argo, 2025), gliders do not need constant management, allowing them to conduct pre-programmed routes and only requiring hands-on input from scientists during their deployment and recovery. This enables them to operate independently from costly research vessels and cover larger regions than ever before. At the same time, gliders offer access to regions previously inaccessible to ship-based measurements - they can approach within 50 meters of icebergs to take measurements of water around these icebergs without the disturbance associated with large vessels (Zhou, Bachmayer, and deYoung, 2019). Gliders can be fitted with a wide range of sensors, such as 3D scanning and sonar mapping sensors (Zhou, Bachmayer, and deYoung, 2019; Zhou, Bachmayer, and Young, 2014); conductivity, temperature and depth sensors; acoustic fish and mammal detection; and optical sensors used to record fluorescence and other biological properties of the water (Jasco, 2024; Brearley et al., 2024). The combination of high-precision data combined with control of the position of the glider, a feature lacking on platforms such as the Argo floats, makes gliders suitable for a wide range of oceanographic studies.

Unfortunately, gliders are not without flaws: slow speeds and poor manoeuvrability make them vulnerable to strong currents (Song et al., 2020), while

space and energy constraints can limit the options for science payloads. Bubbles also present a problem for gliders utilising optical sensors, particularly sensors calculating volume backscattering functions to calculate the turbidity of the water. For these sensors, bubbles refract the light in a similar way to particles but the relation between volume scattering function and concentration is different, preventing accurate conversion. It is important to confirm that the volume scattering functions do not contain signals from bubbles to ensure the conversion to particle concentrations is reliable. In order to ascertain whether productivity around Discovery Bank is affected by Taylor columns, we first need to investigate whether the effects of bubbles on backscattering data can be mitigated. This thesis will suggest a method for reducing the erroneous high readings received from bubbles based on the difference from other nearby unaffected readings.

2. Literature Review

2.1. History of Gliders

Gliders were first proposed as an alternative to propeller-driven underwater vehicles in the early 1960s by Concept Whisper, an American military project constructed by General Dynamics aiming to provide a method of transporting military troops silently through the ocean (Jenkins et al., 2003). The concept of buoyancy gliders was patented by Ewan Fallon (Fallon, 1965), proposing the sawtooth profile used by modern gliders, driven by a buoyancy engine. The potential uses of buoyancy gliders remained purely military until the late 1980s when oceanographer Henry Stommel proposed a fleet of gliders to conduct oceanographic research, nicknamed “The Slocum Mission” (Stommel, 1989). The project was named after Joshua Slocum, the first person to single-handedly sail around the world, indicating the global vision that Henry Stommel had for this project. In 1992 the University of Tokyo introduced ALBAC, a drop weight glider that was only capable of a single glider cycle (Javaid et al., 2014). In the late 1990s the US Office of Naval Research produced three different gliders: Seaglider, Spray and Slocum (Petritoli and Leccese, 2024). Produced by the Webb Research Corp (WRC) in collaboration with Henry Stommel (Griffiths et al., 2007), the Slocum glider was initially created for shallow water missions as it was powered by a single stroke pump, whose capacity limited the glider’s operation in deeper water. By 2008, a later edition of the glider, Slocum Thermal, solved these problems by using a Carnot cycle energy recovery system that utilizes the temperature gradient between

deep and surface waters to extract energy (Jenkins et al., 2003). Modern versions of the Slocum Thermal such as the Slocum Sentinel now have endurances of up to 2 years (Teledyne Marine, 2024), but are reliant on strong temperature gradients. These gradients are not necessarily present within the Southern Ocean and therefore a successor of the original Slocum, the Slocum G2 which still uses the buoyancy pump, is used in this study.

2.2. Taylor Columns over the South Scotia Ridge

The Weddell Sea is a region of the Southern Ocean east of the Western Antarctic Peninsula. It contains the Weddell abyssal plain and the Weddell gyre (WG), a large rotating body of water driven by the Antarctic Circumpolar Current (ACC). The South Scotia Ridge is a line of seamounts north of the Weddell sea that separates the Weddell abyssal plain from the Scotia Sea, through which the ACC flows. This area is characterised by reduced stratification, called the Weddell-Scotia Confluence (WSC) (Patterson and Sievers, 1980). The water present in the WSC was initially thought to be created by the mixing of the juxtaposed WG and ACC water (Meredith et al., 2015), although more recent studies suggest more complex mixing methods may be occurring (Bearley et al., 2024; Meredith et al., 2015; Whitworth III et al., 1994).

Recent research has investigated the unusual stratification found within this region, where a mid-depth (around 200-400 m) stratification minimum implies entrainment of shelf water into the WSC (Bearley et al., 2024; Whitworth III et al., 1994). Meredith et al. (2015) suggested that this may be caused by stratified Taylor columns that could form around the seamounts found along the South Scotia Ridge. Of particular interest was Discovery Bank, one of the larger seamounts that rises from depths of greater than 5,500 meters from the Weddell Abyssal Plain up to less than 500 meters at its peak (Meredith et al., 2015). This prompted the ORCHESTRA (Ocean Regulation of Climate by Heat and Carbon Sequestration and Transports) project led by BAS to conduct a detailed survey using gliders and floats to investigate the mixing. There is still uncertainty as to the causes of the mixing within Taylor columns, although the accepted consensus is that many seamounts have enhanced diapycnal mixing around the seamounts (Bearley et al., 2024).

The enhanced mixing provided by Taylor Columns is also of great biogeochemical interest. Many studies suggest that regions surrounding Taylor columns have enhanced productivity, due to the upwelling of nutrients, primarily iron, by the Taylor column (Prend et al., 2019; Dower, Freeland, and Ju-

niper, 1992; Huppert, 1975; White, Mohn, and Orren, 1998). There are several competing effects occurring within a Taylor column, although the extent to which they compete is unknown. On the one hand, the retention of water within the column would lead to the depletion of key nutrients and could reduce the region's productivity if those nutrients are limiting. On the other hand, increased diapycnal mixing around the seamounts increases the rate at which nutrients at depth can be transported to the biologically active euphotic zone. This would increase productivity and counteract the reduced productivity caused by the increased water retention. The data analysed in this thesis suggests that there are regions of reduced productivity over the peak of the seamount while the regions around the seamount with strong currents (high depth-averaged velocities) have higher productivity in line with increased diapycnal mixing (Breadley et al., 2024).

2.3. Gliders in the Southern Ocean

The Southern Ocean has long presented difficulties in acquiring data. In the past, data collection has been heavily limited to the austral summer (Graham et al., 2024) as large quantities of ice alongside frequent storms and high winds make ship-based operations hazardous. It is common for just one or two research cruises to take place in the Southern Ocean throughout the entire austral winter (June to September) (Graham et al., 2024). Costs and logistics also present significant barriers to research within the Antarctic Region. With research vessels costing upwards of \$100,000 per day (Cressey, 2024) and requiring extensive coordination and collaboration, gliders provide a lower-cost method to retrieve data from a wide area while maintaining good spatial resolution, accurate data and reliable results (Petritoli and Leccese, 2024). Because of these factors, gliders were quickly adopted by Southern Ocean researchers, first being used around Antarctica by Rutgers' Institute of Marine and Coastal Sciences' Coastal Ocean Observation Laboratory (COOL) in 2007 (Jones and Webb, 2007). After extensive winter testing offshore of New Jersey, COOL sent a Slocum glider on a 23-day mission from near Palmer Research station to be collected near Rothera station, "going where no glider has gone before" (Jones and Webb, 2007, p.4). This mission proved that gliders could handle low temperatures, Antarctic megafauna, navigate icebergs, and deal with the many other challenges associated with operating within high latitude environments (Jones and Webb, 2007). By proving the feasibility of buoyancy gliders in this environment, this mission catalysed the use of gliders in the

Southern Ocean (Schofield et al., 2024). The long ranges of Slocum gliders, up to 40,000 km (Javaid et al., 2014), makes them suitable for long-term missions through the austral winter. From 2012 onwards, projects such as the British Antarctic Survey's (BAS) Rothera time series (RaTS) (Venables et al., 2023) and the Palmer Long Term Ecological Research began frequent use of gliders to supplement existing ARGO floats and ship-based measurements (Schofield et al., 2024) in the Southern Ocean, initially focused around the Western Antarctic Peninsula. Since then, projects such as the Gliders: Exciting New Tools for Observing the Ocean (GENTOO) project have introduced gliders into the Weddell Sea (Biddle et al., 2015).

2.4. Glider Data

Giders allow a range of different measurements to be taken within the Southern Ocean. Conductivity, temperature and depth (CTD) sensors enable the identification of the origin of different water masses (Breadley et al., 2024) while optical sensors allow for the measurement of a variety of different biological properties of seawater such as chlorophyll, phyco-cyanin and fluorescein concentrations as well as indicating the quantities of particulate matter within the water. A significant problem with glider-based data is the effect of bubbles on particulate matter measurements. Particulate matter is recorded using an optical backscattering sensor where offset optical emitters and sensors record the fraction of light scattered by particulate matter. The volume backscattering function is significantly affected by the presence of bubbles on the optical sensor as the signal returned by bubbles is indistinguishable from high levels of particulate matter within the water sample, as confirmed by studies such as Miles et al. (2015), where rough sea conditions generated by Hurricane Sandy led to high readings of particulate backscattering coefficient (b_{bp}) near the surface. These bubbles cause significant issues after resurfacing - important given that, in the UK ORCHESTRA project, the glider resurfaced after every dive. This led to significantly higher b_{bp} values present in the top 80 to 100 meters of the downcast of each dive, visible as stripes within the raw data. Previous studies have either not addressed this problem (Davis et al., 2008) or simply removed the affected readings (Gentil et al., 2020; Glenn et al., 2008; Hendrikx Freitas et al., 2016). This problem affects all our data so a novel approach is required to preserve the integrity of the data. This study uses upcasts close to affected downcasts to adjust the downcast readings to minimise the difference between the two directions, allowing all downcast data to be used.

3. Data

3.1. Location Selection and Data Acquisition

The glider data presented here was acquired as part of the UK ORCHESTRA programme in early 2019 on a Teledyne Webb Research Slocum G2 glider deployed from the RRS James Clark Ross. This region was selected to investigate the water transformation in the WSC, but the bio-optical data collected has not yet been analysed. The glider deployment began on 2nd February 2019 at the location shown in Figure 1. The glider was active until the 9th of April, having made six complete crossings of Discovery Bank, the largest seamount in the South Scotia Ridge (Breadley et al., 2024).

This thesis will primarily examine bio-optical data from the fifth and sixth passes, starting from the location where the fifth pass began and ending when the sixth pass reached the same location. The fifth pass is labelled Transect 1 and represents the path from the tip of the seamount out to the deepest area surrounding the mount. Transect 2 is pass six, when the glider returns to the seamount. Transects 1 and 2 were chosen to provide a full cross-section of the seamount/Taylor column system and are used to illustrate the effects of bathymetry on productivity. To mitigate the risk of the glider colliding with the sea floor some profiles within these transects do not extend down to the target depth of 1000 meters. Therefore, Transect 3 was created as a subset of Transects 1 and 2 where chlorophyll and b_{bp} data was reliably recorded down to 1000 meters and is used as a clear example of the effects of the data processing steps described in this thesis.

The glider was fitted with a CTD sensor, dissolved oxygen optode, photosynthetically active radiation (PAR) sensor and a WETLabs EcoPuck containing a coloured dissolved organic matter (CDOM) sensor, an optical backscattering sensor and a fluorometer recording chlorophyll concentrations (Breadley, 2019). The CTD data was compared and corrected against high-quality CTDs. Full details of the temperature and salinity corrections can be found in Breadley et al. (2024). The corrected CTD data was used for the calculation of the mixed layer depth (MLD) as well as conversion of volume backscattering function to the particulate backscattering coefficient. The PAR data was used for the calculation of photic depth, using the method in Lee et al. (2007). Data from the dissolved oxygen optode and CDOM is not used here.

The majority of the data analysed in this thesis comes from the EcoPuck. The EcoPuck's fluorometer excites chlorophyll with 470 nm light, which fluoresces to produce light that is detected at 695 nm. This is linearly correlated with chlorophyll concentration and scaling is used to convert the voltage received from the optical sensor to a concentration in $\mu\text{g l}^{-1}$. This takes place aboard the glider. The backscattering sensor uses a light source offset at 124° from an optical sensor to estimate the total backscattering of the water. Factors influencing the degree to which a sample of water scatters lights include attributes of the water itself, suspended particles, dissolved particles and air bubbles. Attenuation due to dissolved materials is negligible within the red part of the optical spectrum, so light at 700 nm is used (Consoritium for Ocean Leadership, 2023). Bathymetry data used in this thesis is sourced from the GEBCO 2024 15 arcsecond dataset (GEBCO, 2024).

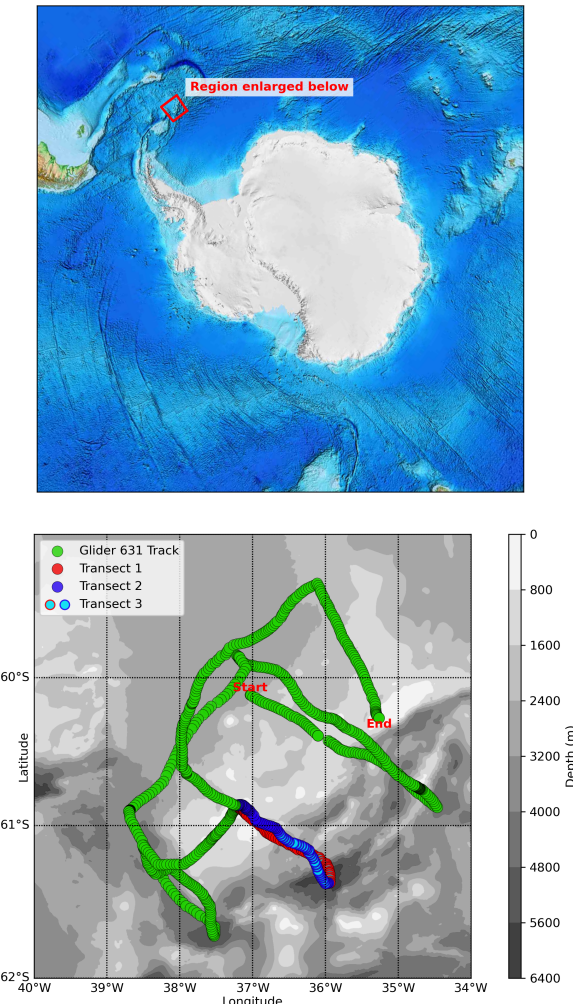


Figure 1: Location and Map of glider path. Red markers denote the data used for Transect 1, a path from the top of the seamount to the deepest contour. Dark blue markers denote Transect 2, the return transect. A subset of Transect 1 and 2, Transect 3 is marked with an additional cyan dot.

3.2. Initial Data Manipulation

The data was processed within Python, primarily utilising Pandas (written in C) for efficiency. The entire dataset was imported as a single, continuous dataframe, before being split into a sequence of profiles (with unique profiles for each up and downcast), each containing their own dataframe with several custom methods for ease of manipulation and to minimise data loaded in memory. Data was cached after significant preprocessing steps to reduce computation time. General functions were written to be applied to a generic list of profiles. This means the code could be very easily modified for use with other datasets. Based on profile indicies generated by the glider, the data could be split into transects representing the different paths and locations the glider traversed, labelled on Figure 1.

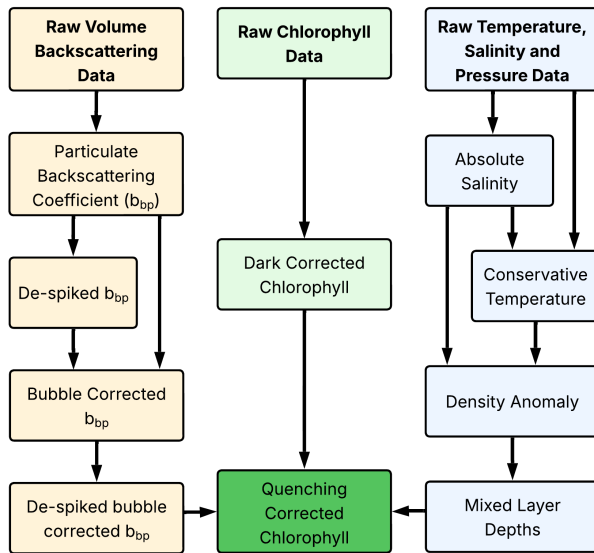


Figure 2: Flowchart of data processing steps.

Before the glider data could be used, the following preprocessing steps needed to be taken:

- Calculation of accurate salinity and temperature readings.
- Mixed layer depth calculation via density anomaly.
- Conversion of volume backscattering function into particulate backscattering coefficient (b_{bp}).
- Sanitisation of the resulting b_{bp} data using de-spiking and bubble correcting.
- Dark correcting chlorophyll data.
- Combining the b_{bp} , mixed layer depth and chlorophyll data as part of the chlorophyll quenching correction.

Once these steps (in Figure 2 and detailed below) had been completed, the resulting quenching corrected chlorophyll data could be analysed.

4. Methodology and Results

4.1. Calculation of accurate temperature and salinity readings.

Salinity and temperature were quality-controlled according to the process used in Brearley et al. (2024), after which the publicly available ‘GSW’ module based on the TEOS-10 equations (Intergovernmental Oceanographic Commission, 2010) was used in Python to convert the practical salinity into absolute salinity and the temperature into conservative temperature used for the mixed layer depth calculations.

4.2. Conversion of Volume Backscattering Function to b_{bp} .

The relation between the volume scattering function, β , and b_{bp} is linear, with the correlation coefficient, $\chi = 1.077$ (Sullivan et al., 2013).

$$b_{bp} = 2\pi\chi(\beta - \beta_{sw}) \quad (1)$$

β_{sw} , the background volume scattering coefficient of seawater, was calculated using the method described in Zhang, Hu, and He (2009), using corrected local temperature and salinity values with the default depolarisation ratio of $\delta = 0.039$. This required the rewriting of the MATLAB scripts from Zhang, Hu, and He (2009) into Python, allowing the quick conversion of to b_{bp} .

4.3. b_{bp} Despiking

The b_{bp} data contains spikes caused by particles in the water. To remove these, an approach similar to Briggs et al. (2011) was used, whereby a 7-point running minimum filter followed by a 7-point running maximum was used to obtain the background readings. Some missing readings within the b_{bp} dataset could not be interpolated, while large amounts of noise was also present. However, once the data was de-spiked, a simple linear interpolation over the missing values was applied.

The subsequent de-spiked dataset was then subtracted from the raw data to obtain the isolated spikes (Figure 3). Subsequently, a noise threshold was obtained as $8.7 \times 10^{-5} \text{ m}^{-1}$, equivalent to the 90th percentile of the entire dataset below 300 meters. Noise from the sensor present in the spike dataset was removed by setting any values smaller than the noise threshold to zero to allow the spikes to be isolated. The spike data can be utilised in the future to investigate the fluxes of sinking particulate matter.

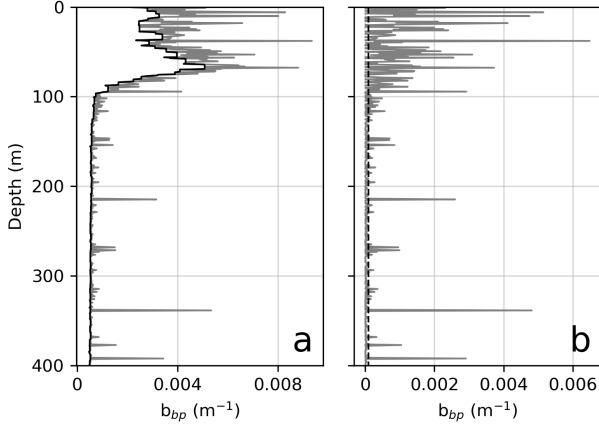


Figure 3: Despiking process. (a) Raw b_{bp} data in grey with the despiked result in black. (b) isolated spikes in grey with the noise threshold of $8.7 \times 10^{-5} m^{-1}$ as a dotted black line.

4.4. Methods for Removing Bubbles

There is a significant difference in the b_{bp} data between the upcasts and downcasts. Figure 4 shows that the upcasts are lacking the large b_{bp} values present in the top 100 meters of the profile.

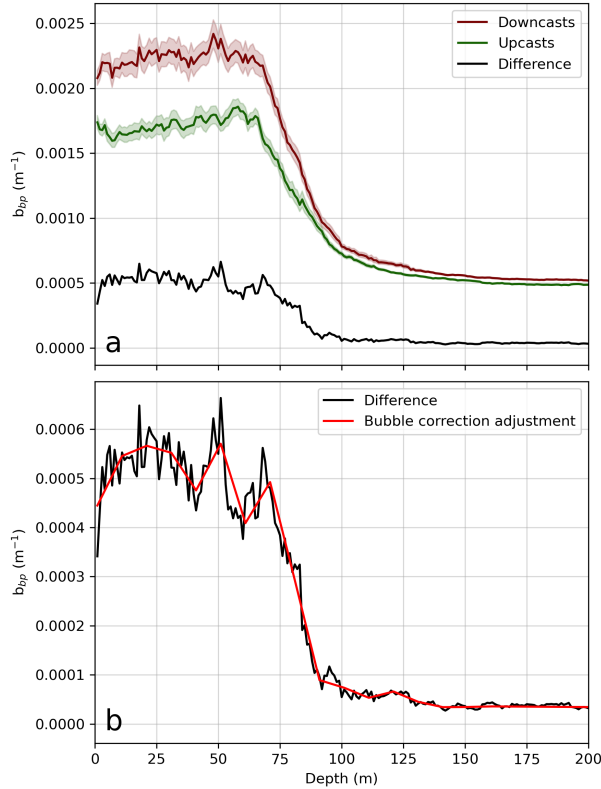


Figure 4: Bubble correction for b_{bp} . (a) b_{bp} plotted against depth for Transect 3 with the shaded region representing the 95% confidence interval. The average difference between up and downcasts is shown in black. (b) Enlarged view of the difference between up and downcasts with an example of the bubble correction adjustment function overlaid in red.

These anomalous datapoints are likely due to air bubbles sticking onto the backscattering sensor and increasing the amount of light scattered into the detector (Briggs, 2025). This discrepancy between the signals persists throughout the entire downcast, although not to a significant degree beyond 80 meters. To remove these signals each (de-spiked) downcast is compared to the mean of the six closest de-spiked upcasts. A piecewise function consisting of multiple linear segments is fitted to the difference between the downcast and its closest upcasts:

$$f(x, y) = y(i) + (y(i+1) - y(i)) \times \frac{x - d(i)}{d(i+1) - d(i)} \quad \{d(i) < x \leq d(i+1)\} \quad (2)$$

$$d = [0, 10, 20, \dots, 150, 160, 999]$$

x is the depth while d is an array of depths for the linear segments. This function is repeated for $i = 0$ to $i = 15$ such that a correction is created for the entire profile. The values of $y(i)$ are initially set to the values of b_{bp} at the locations $d(i)$ but are then optimised (bound to positive values) to create the bubble correction adjustment. This corresponds to a series of sequential linear fits of the data at ten-meter intervals between zero and 160 meters, as well as a single adjustment between 160-999 meters. The locations of these line segments were chosen to allow for high flexibility in the top 160 meters (twice the depth at which the discrepancies are commonly seen) while preventing overfitting in the lower 840 meters. An example of this is shown in Figure 4 (b).

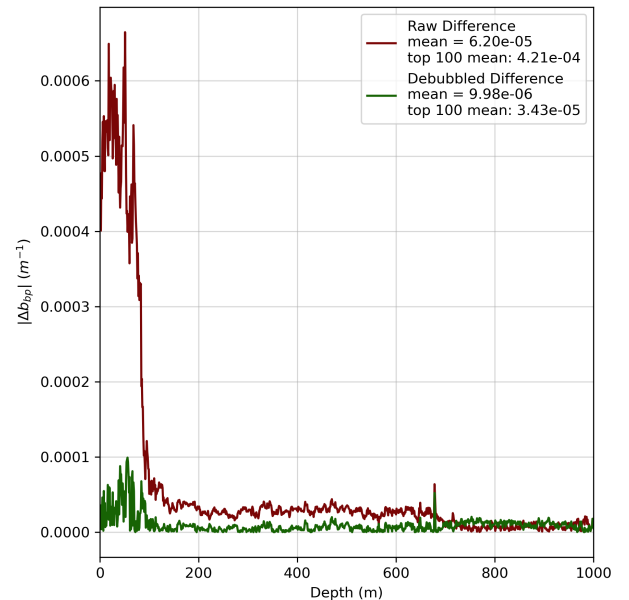


Figure 5: Difference between up and downcast b_{bp} . Data shown is for Transect 3, both before (red) and after (green) the bubble correction. High frequencies are retained while the large discrepancies in the top 100 meters are significantly reduced.

This function is then subtracted from the raw b_{bp} downcast which is then re-run through the despiking process to obtain de-spiked, de-bubbled data. The result of this process was a factor of six reduction in mean discrepancy between the up and downcasts, which increased to over ten within the top 100 meters, as seen in Figure 5. Additionally, within Figure 6 (b) visible stripes are seen between consecutive up and downcasts, while within Figure 6 (c) these stripes are significantly reduced. This difference is most visible within the top 100 meters where the majority of change is seen between the raw and de-bubbled data.

Some sensitivity analysis was conducted on both the length of the segments in the bubble adjustment and the number of upcasts used to compare against

the downcast. Ten-meter segments provided a balance between efficiency of function optimization and good results within the top 100 meters - longer segments resulted in worse fits with the upcast data while shorter segments resulted in overfitting and significantly longer computation times. If fewer than six upcasts were used for comparison, variability in the difference function was high and optimisation did not always return an accurate fit. When more upcasts were used in the comparison, changing conditions were no longer accurately represented in the downcast data. Therefore the smallest number of upcasts that did not create excessive variability, six, was chosen.

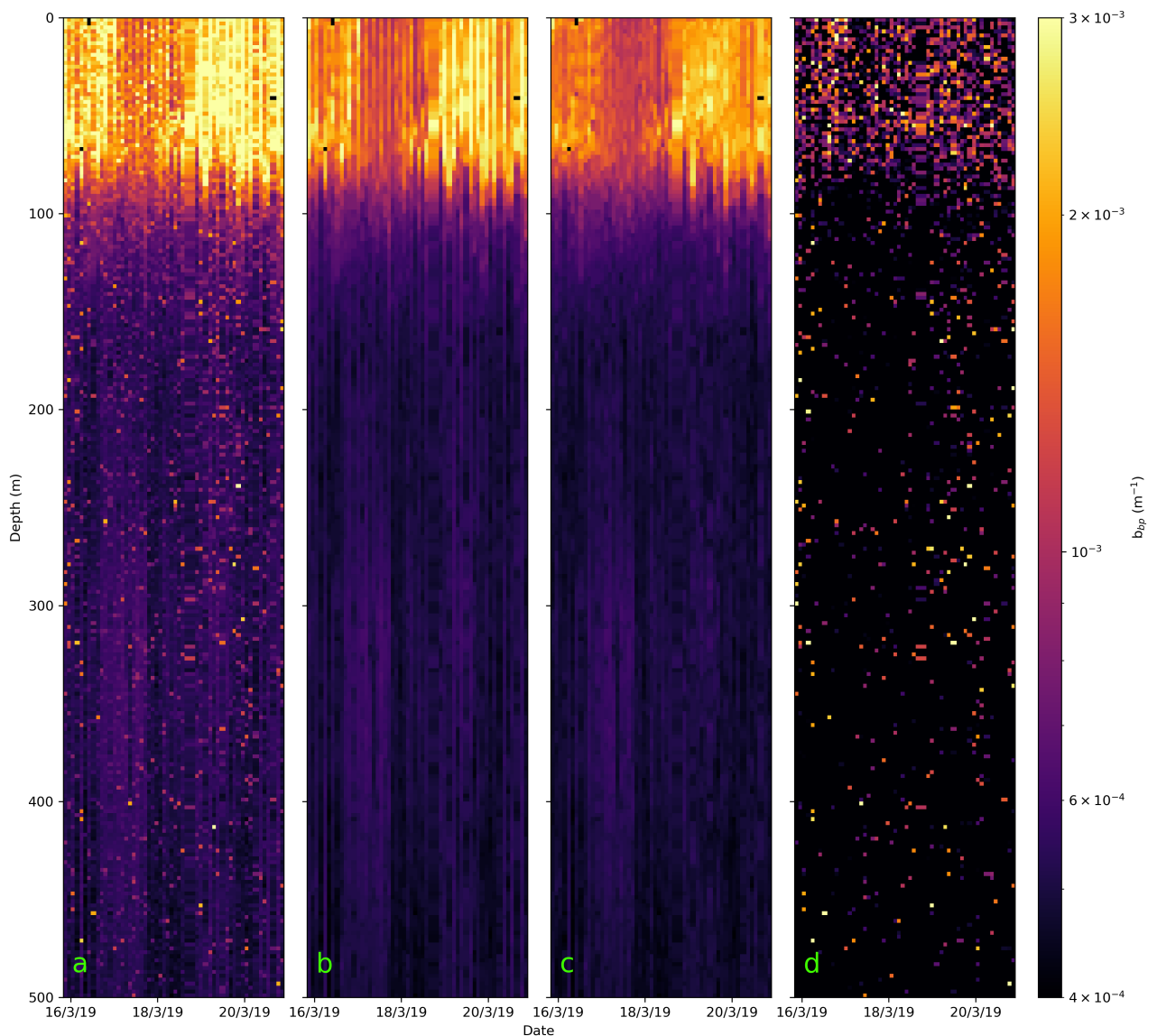


Figure 6: b_{bp} correction stages. Transect 3, gridded to two meter intervals. (a) Raw data, before pre-processing. (b) Despiked data. (c) Despiked data following the bubble correction. (d) The noise-filtered spikes extracted from the final despiking process.

4.5. Chlorophyll Deep Correction

As the chlorophyll data are determined from a scaled voltage, a correction to the deep values where chlorophyll is expected to be zero is required. To do this, a deep correction derived from Thomalla et al. (2018) is used whereby the 5th percentile of chlorophyll below 300 meters is subtracted from the entire column (Figure 7). 300 meters is well below the photic zone where most chlorophyll is found and taking the 5th percentile preserves spikes caused by sinking biological matter. This generates a small number of negative chlorophyll values which are subsequently set to zero.

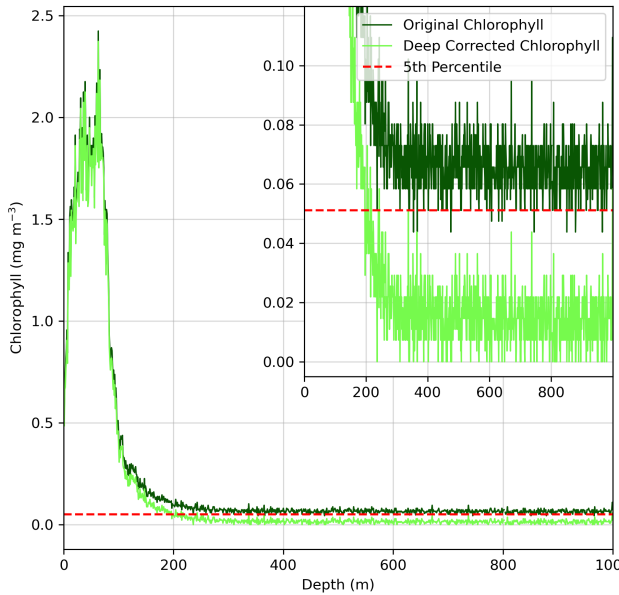


Figure 7: Deep chlorophyll correction. (main) Chlorophyll concentrations for a profile within Transect 1 before and after the deep correction was applied. (inset) Enlarged view of the same profile, showing the position of the 5th percentile below 300 meters at 0.0511 mg m^{-3} .

4.6. Mixed Layer Depth Calculations

Required for the following chlorophyll quenching correction, the MLD is defined as the point within a profile at which the density anomaly is greater than 0.03 kg m^{-3} compared to the density at the surface (Boyer Montégut et al., 2004). The surface density was taken as the first reading when the profile was sorted by depth. Density anomaly was calculated using TEOS-10 calculations applied to the absolute salinity, conservative temperature and pressure (Intergovernmental Oceanographic Commission, 2010). The MLDs were precisely defined as the depth halfway between two data points, where the first is below the 0.03 kg m^{-3} threshold while the second is above. It was decided that 0.03 kg m^{-3} was a valid choice for the MLDs, as this value fell within a region

where the derivative of density anomaly with depth was high - significant changes to the 0.03 kg m^{-3} coefficient would be needed to have any meaningful effect on the calculated MLDs. This can be seen in Figure 8 where the line at 0.03 kg m^{-3} is in a region where the density anomaly line is steep.

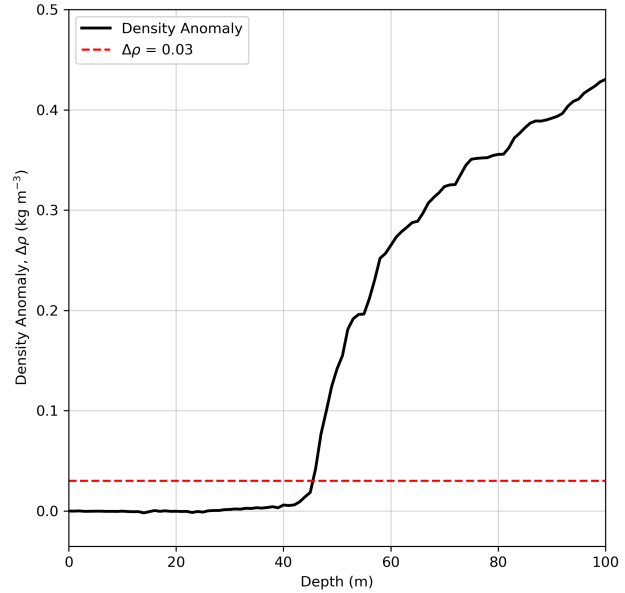


Figure 8: Density anomaly. Density anomaly of the same profile as in Figure 7 . The dashed red line indicates where the density anomaly is 0.03 kg m^{-3} .

4.7. Quenching Correction

In daytime, observed chlorophyll values are often lower than expected within the top 100 meters. This is caused by the photochemical quenching used by phytoplankton to protect themselves from excessive light exposure (Brand, 1982). The premise of the quenching correction is to replace the affected chlorophyll readings with ones derived from the unaffected b_{bp} readings.

To do this, the mean ratio of chlorophyll and bubble corrected, de-spiked b_{bp} within the mixed layer is calculated for the nearest night upcast. This ratio is then multiplied by the b_{bp} data to create a synthetic chlorophyll reading that is not affected by photochemical quenching (Thomalla et al., 2018). Should this correction provide a value that is lower than the original chlorophyll reading the original reading is preserved. This method builds upon that used in Thomalla et al. (2018), the key difference being that instead of applying the chlorophyll to backscatter ratio of the night profile at each depth, the mean ratio of the mixed layer is used. The correction is also applied deeper, across the entire mixed layer.

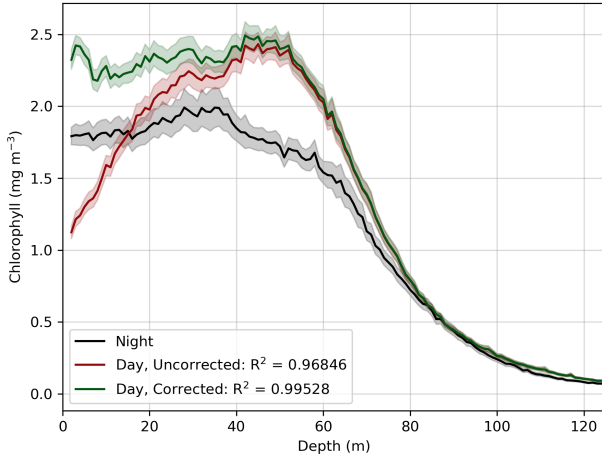


Figure 9: Quenching correction. Chlorophyll concentrations for the uncorrected and corrected day profiles (red and green) compared to the night profiles (black) for the entire dataset. Shaded regions indicate the 95% confidence interval for the respective curve. Correlation coefficients for the day profiles are given with respect to the night profiles.

As can be seen from Figure 9, this quenching correction improved the correlation between the day and night profiles and the corrected day profiles are similar in shape to the night ones. The daytime chlorophyll values derived from the correction are reasonable and in line with expected values for the region. It is expected that the chlorophyll would be more concentrated in the daytime due to the short lifetimes of algae creating diurnal cycles in chlorophyll concentration (Blauw et al., 2018). Within Figure 10 it is evident that the diurnal decrease in chlorophyll concentration within the top 30 meters is no longer present after the correction has been applied.

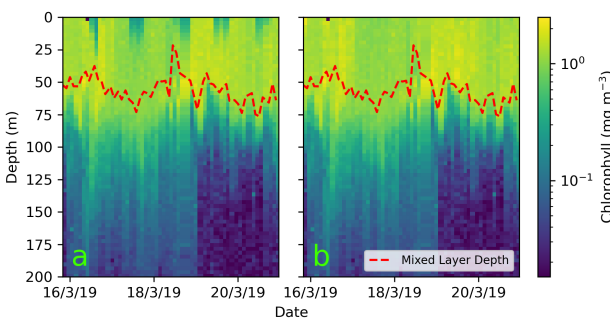


Figure 10: Quenching correction result. Three meter gridded chlorophyll concentrations for Transect 3 before (a) and after (b) the quenching correction is applied. The mixed layer depth is shown as a dotted red line. The daily variation in concentration within the top 30 meters is no longer visible after the correction.

4.8. High Chlorophyll and Photic Zones

To quantify the effect of the Taylor column on the productivity of the region, a number of depths were

calculated. Firstly, the photic depth was calculated as where the photosynthetically active radiation (PAR) fell to 1% of the surface values, interpolating over the night profiles where insufficient PAR was present to calculate the depth. To complement this, the “High Chlorophyll zone” was calculated - defined as the location where chlorophyll fell below 3% of the maximum value within the column, shown in Figure 11. This quantifies the depth to which chlorophyll is present. By computing the difference between the photic depth and High Chlorophyll zone we can determine the locations where additional chlorophyll is present within the water.

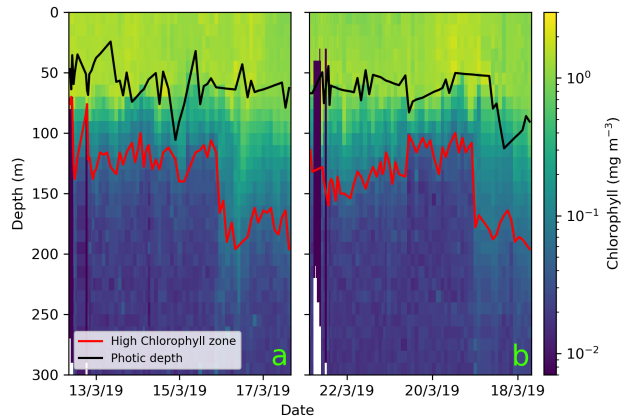


Figure 11: High Chlorophyll zone and photic depths. Ten meter gridded chlorophyll concentrations for (a) Transect 1 and (b) Transect 2 with depth of photic zone (black) and depth of ‘High Chlorophyll zone’ (red). The left edges of the plots corresponds to the tip of the seamount and the centre of the Taylor column.

5. Discussion

5.1. Can the effects of bubbles on backscattering data be mitigated?

The methods described in this paper show that the impact of air bubbles on backscattering data can be effectively mitigated. By using adjustments based on surrounding unaffected profiles the resultant data maintains local variability. The adjustment also takes into account the degree to which bubbles affect the data - if there are few bubbles in the water then there will be little difference between up and downcasts and hence less adjustment. This ensures that it is suitable for long missions where there can be changes in conditions as the seasons change. The ability to prevent bubbles from affecting data is useful in allowing a greater portion of datasets to be used. This proves invaluable when datasets are limited and obtaining more data is not easily feasible, such as when the location is remote, i.e. the Southern Ocean.

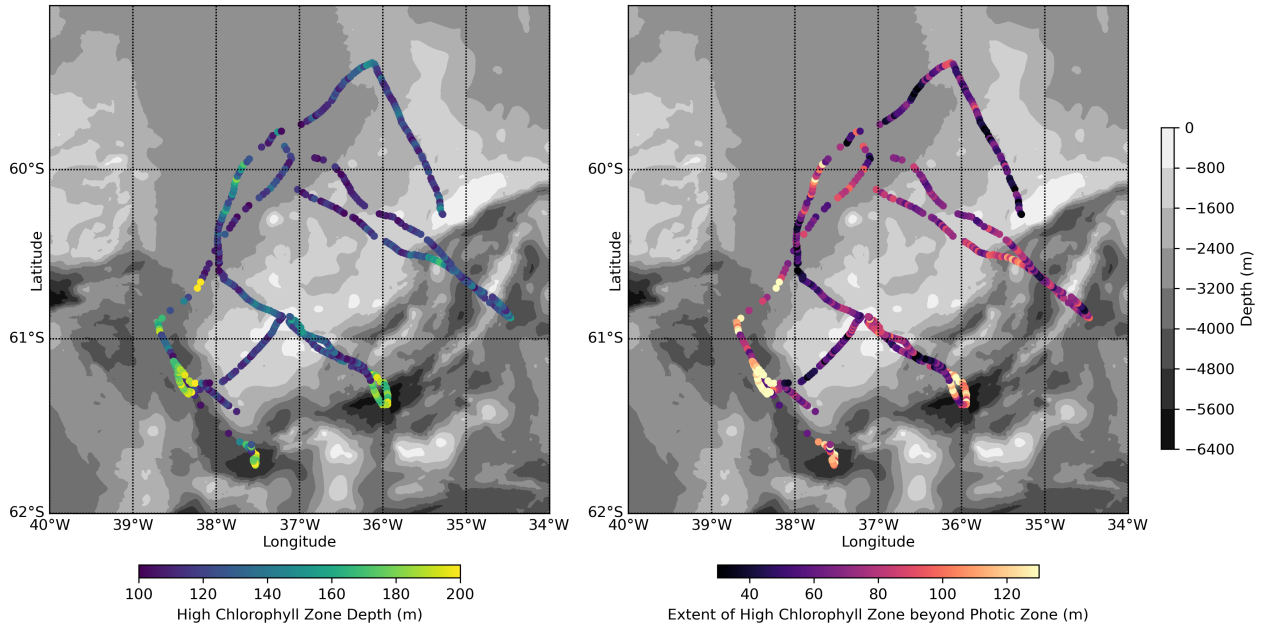


Figure 12: Map of productivity metrics. (left) Map of High Chlorophyll zone depth throughout the glider mission. (right) map of the extent to which the High Chlorophyll zone extends below the Photic Zone depth. GEBCO bathymetry as background.

5.2. Is productivity around Discovery Bank affected by the Taylor column?

Once the effects of bubbles on b_{bp} data was mitigated and chlorophyll quenching corrections applied, it was possible to map the extent to which the high chlorophyll zone extends beyond the photic depth, as shown in Figure 12.

The extent of the high chlorophyll zone beyond the photic depth is used as a proxy to view the effects of increased diapycnal mixing on the water column. The presence of chlorophyll beyond the photic depth likely indicates enhanced vertical mixing within the column. For there to be large quantities of chlorophyll below the photic depth, organic matter must be transported downwards as there is insufficient light for significant algae growth below the photic depth. The exceptions to this would be regions with greatly enhanced b_{bp} (which would correlate with sinking dead organic matter) or regions where a deep chlorophyll maximum (DCM) is present, which would require phytoplankton adapted to low light conditions, common in low-latitude oceans (Boyd et al., 2024). As neither of these are present in the data seen around the seamount, it is reasonable to conclude that the presence of chlorophyll below the photic zone is indicative of enhanced diapycnal mixing.

Figure 12 shows the effect of the seamount (located at 37°W 61°S) on the surrounding region. There are regions where the high chlorophyll zones are significantly deeper than the photic depth around the 3,200 meter contours surrounding the seamount peak. This aligns with the expected boundaries of a

Taylor column predicted by Brearley et al. (2024) as occurring at about the 3,000 meter contours. These high-productivity regions are therefore likely to have increased diapycnal mixing around the boundaries of the Taylor column, increasing the flux of nutrients towards the surface and mixing the existing chlorophyll deeper into the ocean. This is supported by the lower b_{bp} in the surface of these regions, showing that there is more mixing between the particle-dense surface region and the deeper regions with more sparsely distributed particulate matter.

These regions are then contrasted by lower productivity within the centre of the Taylor column. The regions between the 1,600 and 2,400 meter contours do not show enhanced chlorophyll concentrations within the 100 to 200 meter depth region, see Figure 13 (a). This implies the existence of a region with increased water residence times, to the extent that productivity may be limited by nutrient availability. To confirm this, comparisons need to be made to data acquired in the open ocean in a location within minimal underwater features.

It is therefore likely that both processes (increased diapycnal mixing and increased residence times) are present within the Taylor column. In the central region, the lack of nutrients due to the long water residence time is the dominant factor. Conversely, on the boundaries of the column, the residence times are likely shorter, and the diapycnal mixing provides nutrients from the deep while also mixing chlorophyll into the deeper water, which results in deeper regions of high chlorophyll concentrations.

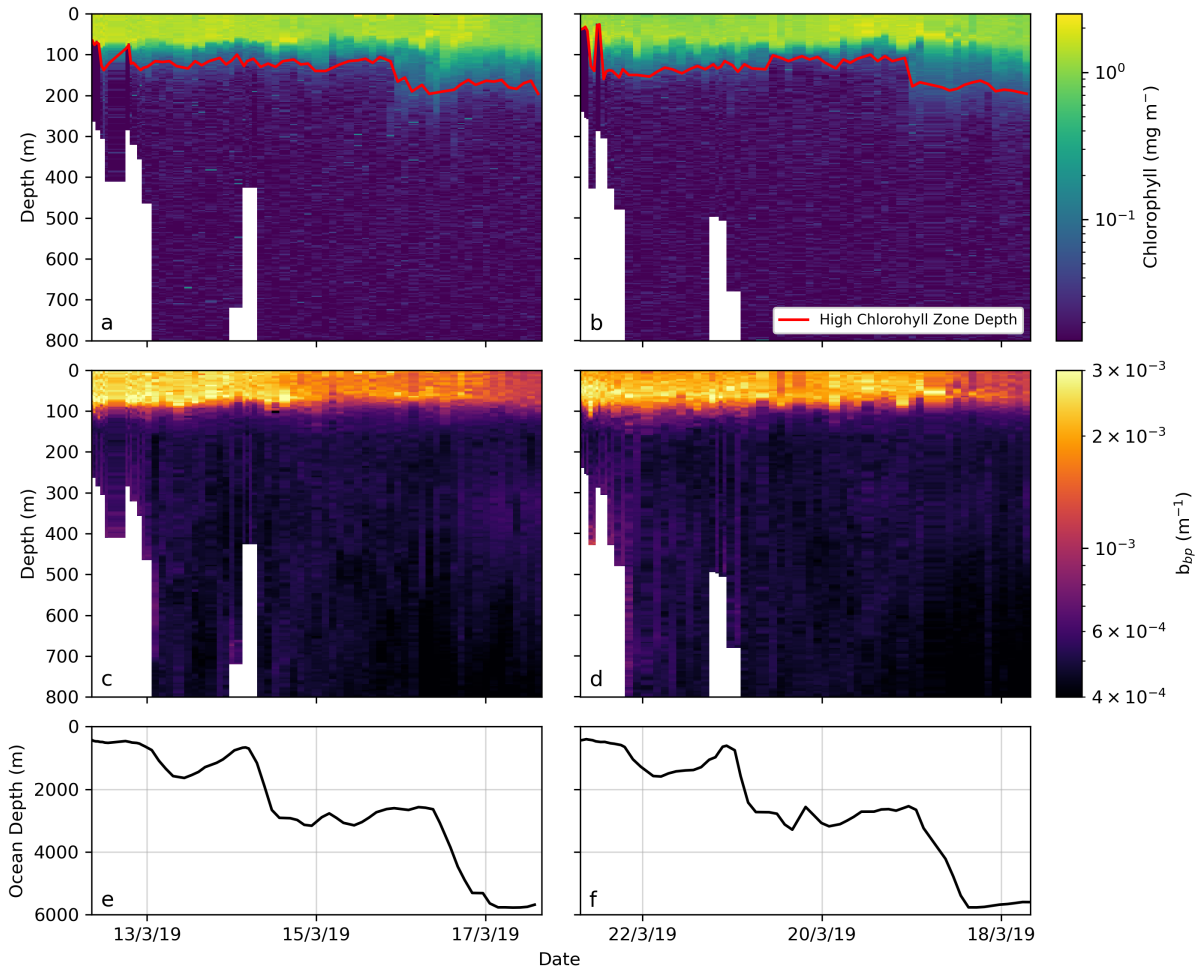


Figure 13: Effects of bathymetry on chlorophyll and b_{bp} . (a, b) Three meter gridded chlorophyll concentration for Transect 1 and 2 respectively. (c, d) Three meter gridded b_{bp} data for Transect 1 and 2 respectively. (e, f) Depth data interpolated from GEBCO bathymetry. The left edges of the plots corresponds to the tip of the seamount and the centre of the Taylor column.

5.3. Future Options

During the cruise, there were unfortunately no water samples taken against which to calibrate biogeochemical data. Bottle samples, either returned to a laboratory or analysed onboard the ship, would have provided a reference reading that we could confirm is unaffected by bubbles. By taking a sample in the same location as a bubble-affected downcast, either at the start or end of the mission, the accuracy of the bubble correction could be quantified. Ascertaining the quality of this bubble correction would be useful before applying it to other datasets. Future studies could confirm this by applying it to datasets where reference samples were taken and analysed in a laboratory.

To help quantify the effects of the Taylor column on water residence times and hence on productivity, chlorophyll within the column could be compared to chlorophyll in the open ocean. If chlorophyll concentrations within the column are significantly lower than in the open ocean it would indicate that the

long residence times are affecting the availability of nutrients within the bounds of the column. This could potentially be conducted using satellite data but preferably would be done using gliders so that the vertical profiles of chlorophyll in nearby open oceans can be compared. Future glider missions could also further elucidate the exact mixing processes occurring in the boundaries of the column. It would be recommended for a glider to revisit the same transects more than once within a deployment to ensure that transient temporal anomalies are not affecting the data. If a longer mission using several sequential glider deployments were to be conducted, the interactions between the different seasons and the Taylor column could be investigated, although sea conditions in the austral winter could cause difficulties in reliably recovering and deploying the gliders. Repeat transects would also allow the comparison of data in the same location over time and enable one to establish a value for the sinking speed of particulate matter and then ascertain a rate at which carbon is sinking in the vicinity of the Taylor column.

5.4. Importance of solving this problem

Accurate measurements of chlorophyll and particulate matter within the ocean are crucial for understanding the rates at which organic matter is sinking. Knowledge of this rate can in turn help determine the efficiency at which the ocean stores carbon and is crucial in guiding climate policy decisions.

Within the particulate backscattering data, bubbles would artificially increase the concentration of particulate matter within the water. When quenching corrections are applied, these incorrectly high readings of b_{bp} would increase the calculated chlorophyll concentrations, thereby overestimating productivity metrics within the photic zone. This could potentially lead to inaccurately low values for the sinking flux of carbon, downplaying the significance of the ocean in global policy decisions regarding climate change. As such the understanding of the effects of bubbles on b_{bp} and chlorophyll data is key in ensuring reliable estimates of carbon sequestration are calculated.

6. Conclusion

The ocean plays a critical role in the global carbon cycle, and oceanographic data drawn from buoyancy gliders can be utilised in informing policy decisions. Gliders present a unique solution to improving the temporal and spatial ranges over which data can be

collected, providing novel insights into the transformations and mixing processes occurring within the ocean. This thesis has shown that errors in particulate backscattering coefficients caused by air bubbles on the bio-optical sensors can be mitigated, reducing the discrepancies between up and downcasts by a factor of six, allowing a greater portion of acquired glider data to be used in analysis. Having mitigated against these errors, the analysis is then able to reveal that the Taylor column above Discovery Bank does affect local productivity. There is strong evidence that there is increased diapycnal mixing within the boundaries of the Taylor column, creating a ring of enhanced productivity around the seamount. Meanwhile, there is also some limited evidence that the centre of the Taylor column has increased water residence times, indicated by the shallower region of high chlorophyll. To further investigate this, comparisons to the open ocean, perhaps using satellite-derived concentrations, would have to be conducted. Overall, Taylor columns clearly affect the local productivity around seamounts and the degree to which this affects the rate of carbon sinking into the deep ocean should be a priority for future investigations. Thus this analysis advances methodologies for glider data processing and provides insights into the impacts of the hydrodynamics surrounding seamounts on biological productivity, with implications for understanding ocean carbon sequestration and informing climate policy.

Acknowledgements

The writing of this thesis would not have been possible without the support of my supervisors, Prof. Kate Hendry and Dr Alex Brearley, who provided invaluable guidance and support throughout the project. I would also like to thank those who provided advice and feedback during the data analysis and write up process, namely Dr Natasha Lucas and Dr Nathan Briggs.

Code and Data Availability

The code used in this analysis is available at: <https://github.com/louis-de-neve/gliders25/tree/main/Louis>
The data used in this analysis is not currently publicly available.

References

- Argo (2025). Argo. Accessed: 2025-05-07. URL: <https://argo.ucsd.edu>.
- Biddle, Louise C et al. (2015). "Ocean glider observations of iceberg-enhanced biological production in the northwestern Weddell Sea". *Geophysical Research Letters* 42.2, pp. 459–465.
- Blauw, Anouk N et al. (2018). "Predictability and environmental drivers of chlorophyll fluctuations vary across different time scales and regions of the North Sea". *Progress in Oceanography* 161, pp. 1–18.
- Boyd, Philip W et al. (2024). "Controls on polar Southern Ocean deep chlorophyll maxima: Viewpoints from multiple observational platforms". *Global Biogeochemical Cycles* 38.3.
- Boyer Montégut, Clément de et al. (2004). "Mixed layer depth over the global ocean: An examination of profile data and a profile-based climatology". *Journal of Geophysical Research: Oceans* 109.C12.
- Brand, LE (1982). "Persistent diel rhythms in the chlorophyll fluorescence of marine phytoplankton species". *Marine Biology* 69, pp. 253–262.
- Brearley, J Alexander (2019). *Cruise Report, RRS James Clark Ross, JR18004, 6th January to 17th February 2019*. Accessed: 2025-05-07. URL: https://www.bodc.ac.uk/resources/inventories/cruise_inventory_reports/jr18004.pdf.
- Brearley, J Alexander et al. (2024). "Mixing and water mass transformation over discovery bank, in the Weddell-Scotia confluence of the Southern Ocean". *Journal of Geophysical Research: Oceans* 129.9.
- Briggs, Nathan (2025). "Private Correspondence". 2025-03-14.
- Briggs, Nathan et al. (2011). "High-resolution observations of aggregate flux during a sub-polar North Atlantic spring bloom". *Deep Sea Research Part I: Oceanographic Research Papers* 58.10, pp. 1031–1039.
- Consortium for Ocean Leadership (2023). *Data Product Specification for Optical Backscatter*. Accessed: 2025-05-07. URL: https://oceanobservatories.org/wp-content/uploads/2023/09/1341-00540_Data_Product_SPEC_FLUBSCT_OOI.pdf.
- Cressey, Daniel (2024). *Scientists are becoming ocean hitchhikers to fill data gaps*. Accessed: 2025-05-07. URL: <https://dialogue.earth/en/ocean/scientists-are-becoming-ocean-hitchhikers-to-fill-data-gaps>.
- Davis, Russ E et al. (2008). "Glider surveillance of physics and biology in the southern California Current System". *Limnology and Oceanography* 53.5.2, pp. 2151–2168.
- DeVries, Tim (2022). "The ocean carbon cycle". *Annual Review of Environment and Resources* 47.1, pp. 317–341.
- Dower, John, Howard Freeland, and Kim Juniper (1992). "A strong biological response to oceanic flow past Cobb Seamount". *Deep Sea Research Part A. Oceanographic Research Papers* 39.7-8, pp. 1139–1145.
- Ellison, Elizabeth (2023). "Multi-time scale control of Southern Ocean diapycnal mixing over Atlantic tracer budgets". *Climate Dynamics* 60.9, pp. 3039–3050.
- Eppley, Richard W, Edward H Renger, and Peter R Betzer (1983). "The residence time of particulate organic carbon in the surface layer of the ocean". *Deep Sea Research Part A. Oceanographic Research Papers* 30.3, pp. 311–323.
- Fallon, Ewan (1965). *Hydroglider*. U.S. Patent 3 204 596 (A), Sept. 1965.
- Fuentes, OU Velasco (2009). "Kelvin's discovery of Taylor columns". *European Journal of Mechanics-B/Fluids* 28.3, pp. 469–472.
- GEBCO (2024). *GEBCO Bathymetry Download*. Accessed: 2025-05-07. URL: <https://download.gebco.net>.
- Gentil, Mathieu et al. (2020). "Glider-based active acoustic monitoring of currents and turbidity in the coastal zone". *Remote Sensing* 12.18, p. 2875.
- Glenn, Scott et al. (2008). "Glider observations of sediment resuspension in a Middle Atlantic Bight fall transition storm". *Limnology and Oceanography* 53.5.2, pp. 2180–2196.
- Graham, Myrah et al. (2024). "New methods of undertaking marine science in Antarctica using tourism vessels". *PLOS Climate* 3.2.
- Griffiths, Gwynn et al. (2007). "Undersea gliders". *Journal of Ocean Technology* 2.2, pp. 64–75.
- Henderikx Freitas, Fernanda et al. (2016). "Assessing controls on cross-shelf phytoplankton and suspended particle distributions using repeated bio-optical glider surveys". *Journal of Geophysical Research: Oceans* 121.10, pp. 7776–7794.
- Huppert, Herbert E (1975). "Some remarks on the initiation of inertial Taylor columns". *Journal of Fluid Mechanics* 67.2, pp. 397–412.
- Intergovernmental Oceanographic Commission (2010). *The international thermodynamic equation of seawater – 2010*. Accessed: 2025-05-07. URL: https://teos-10.org/pubs/TEOS-10_Manual.pdf.
- Jasco, Jasco Applied Sciences (2024). "A fleet of Slocum gliders equipped with OceanObserver™ systems successfully demonstrated the ability to detect and localize marine mammals off the Coast of Nova Scotia". Accessed: 2025-05-07. URL: <https://www.jasco.com/news/2024/slocum-gliders->

- detect-and-localize-marine-mammals-off-north-coast.
- Javaid, Muhammad Yasar et al. (2014). "Underwater gliders: a review". *MATEC web of conferences*. Vol. 13. EDP Sciences, p. 02020.
- Jenkins, Scott A et al. (2003). "Underwater glider system study". Scripps Institution of Oceanography Technical Report No. 53.
- Jones, Clayton and Doug Webb (2007). "Slocum gliders—advancing oceanography". *Proceedings of the 15th International Symposium on Unmanned Untethered Submersible Technology conference (UUST-07)*. Vol. 15.
- Lee, ZhongPing et al. (2007). "Euphotic zone depth: Its derivation and implication to ocean-color remote sensing". *Journal of Geophysical Research: Oceans* 112.3.
- Meredith, Michael P et al. (2015). "Circulation, retention, and mixing of waters within the Weddell-Scotia Confluence, Southern Ocean: The role of stratified Taylor columns". *Journal of Geophysical Research: Oceans* 120.1, pp. 547–562.
- Miles, Travis et al. (2015). "Glider observations and modeling of sediment transport in Hurricane Sandy". *Journal of Geophysical Research: Oceans* 120.3, pp. 1771–1791.
- Patterson, Steven L and Hellmuth A Sievers (1980). "The Weddell-Scotia Confluence". *Journal of Physical Oceanography* 10.10, pp. 1584–1610.
- Petritoli, Enrico and Fabio Leccese (2024). "Autonomous Underwater Glider: A Comprehensive Review". *Drones* 9.1, p. 21.
- Prend, Channing J et al. (2019). "Physical drivers of phytoplankton bloom initiation in the Southern Ocean's Scotia Sea". *Journal of Geophysical Research: Oceans* 124.8, pp. 5811–5826.
- Schofield, Oscar et al. (2024). "Buoyancy Gliders Opening New Research Opportunities in the Southern Ocean". *Marine Technology Society Journal* 58.1–2, pp. 26–37.
- Song, Lijun et al. (2020). "Research on negative-buoyancy autorotating-rotor autonomous underwater vehicles". *Applied Ocean Research* 99, p. 102123.
- Stommel, Henry (1989). "The Slocum Mission". *Oceanography* 2.1, pp. 22–25.
- Sullivan, James M et al. (2013). "Measuring optical backscattering in water". *Light scattering reviews* 7, pp. 189–224.
- Teledyne Marine (2024). *Slocum Sentinel Glider*. Accessed: 2025-05-07. URL: <https://www.teledynemarine.com/en-us/products/SiteAssets/Webb%20Research/Teledyne%20Marine%20Slocum%20Sentinel%20Glider%20Data%20Sheet%202025.pdf>.
- Thomalla, Sandy J et al. (2018). "An optimized method for correcting fluorescence quenching using optical backscattering on autonomous platforms". *Limnology and Oceanography: Methods* 16.2, pp. 132–144.
- Venables, Hugh et al. (2023). "Sustained year-round oceanographic measurements from Rothera Research Station, Antarctica, 1997–2017". *Scientific Data* 10.1, p. 265.
- Vives, Clara R et al. (2022). "Iron and light limitation of phytoplankton growth off East Antarctica". *Journal of Marine Systems* 234, p. 103774.
- White, Martin, Christian Mohn, and MJ Orren (1998). "Nutrient distributions across the Porcupine Bank". *ICES Journal of Marine Science* 55.6, pp. 1082–1094.
- Whitworth III, T et al. (1994). "Weddell Sea shelf water in the Bransfield Strait and Weddell-Scotia confluence". *Deep Sea Research Part I: Oceanographic Research Papers* 41.4, pp. 629–641.
- Zhang, Xiaodong, Lianbo Hu, and Ming-Xia He (2009). "Scattering by pure seawater: Effect of salinity". *Optics express* 17.7, pp. 5698–5710.
- Zhou, Mingxi, Ralf Bachmayer, and Brad de Young (2019). "Mapping the underside of an iceberg with a modified underwater glider". *Journal of Field Robotics* 36.6, pp. 1102–1117.
- Zhou, Mingxi, Ralf Bachmayer, and Brad de Young (2014). "Working towards seafloor and underwater iceberg mapping with a Slocum glider". *2014 IEEE/OES Autonomous Underwater Vehicles (AUV)*. IEEE, pp. 1–5.